Indication of the onset of collectivity in ^{30}P

Indrani Ray,[1] Moumita Roy Basu,[2] Ritesh Kshetri,[1] Maitreyee Saha Sarkar,[1,*] S. Sarkar,[3] P. Banerjee,[1] S. Chattopadhyay,[1] C. C. Dey,[1] A. Goswami,[1] J. M. Chatterjee,[1] A. Mukherjee,[1] S. Bhattacharya,[1] B. Dasmahapatra,[1] P. Datta,[4] H. C. Jain,[5] R. K. Bhowmik,[6] S. Muralithar,[6] and R. P. Singh[6]

[1]*Saha Institute of Nuclear Physics, 1/AF, Bidhannagar, Kolkata-700064, India*
[2]*University of Calcutta, 87 /1 College Street, Kolkata-700073, West Bengal, India*
[3]*Department of Physics, Bengal Engineering and Science University, Shibpur, Howrah-711103, India*
[4]*Department of Physics, Anandamohan College, Kolkata-700009, India*
[5]*Tata Institute of Fundamental Research, Mumbai-400005, India*
[6]*Inter-University Accelerator Centre, Aruna Asaf Ali Marg, New Delhi-110067, India*

(Received 15 February 2007; published 18 September 2007)

^{30}P has been studied by in-beam γ-spectroscopy following the fusion-evaporation reaction ^{16}O(^{16}O,pn) at $E_{\rm lab} = 40$ MeV, using the Indian National Gamma (Clover) Array (INGA) up to moderate spins ($I = 5$). Polarization measurements of seven gamma rays have been performed for the first time. To understand the underlying structure of the levels and transition mechanisms, experimental data have been compared with the results from large basis cross-shell shell model calculations. The results for the negative parity states are especially important in this respect. Positive parity states indicate an onset of collectivity, whereas the negative parity states are members of ν-π multiplets.

DOI: 10.1103/PhysRevC.76.034315 PACS number(s): 23.20.Lv, 23.20.En, 21.60.Cs, 27.30.+t

I. INTRODUCTION

The self-conjugate nucleus ^{30}P having seven valence protons and the same number of neutrons with respect to the ^{16}O inert core is in the middle of the sd shell. Apart from the single particle excitations, the spectroscopy of several nuclei in this mass region revealed deformed states, even superdeformation, at low-excitation energies, indicating that these nuclei can easily lose sphericity [1]. For ^{30}P, the number of low-lying configurations which can mix is expected to be sufficient to make highly configuration mixed states more probable. So the onset of collectivity might be expected in ^{30}P and it is interesting to study the evolution of collectivity in it, manifested in terms of large configuration mixing in the shell model calculations.

Recent studies indicate that for some nuclei (^{35}Cl [2], ^{34}P, ^{36}S [3], etc.) in this region, intruder configurations from the neighboring fp shell become important. It is shown that in shell model calculations, in order to reproduce the negative parity and high spin positive parity excited states in ^{35}Cl, ^{34}P, and ^{36}S, the single particle energies (spes) of the fp orbitals have to be reduced by about 3–5 MeV. This implies that for these nuclei, the sd and fp shells come closer, i.e., there is a reduction in the sd-fp shell gap. The occurrence of low-lying intruder orbitals has been shown to be due to the residual intershell and intrashell strong interactions [4]. Using the example of stable calcium isotopes [5], it has been argued that the erosion of the shell closure is related to cross-shell proton-neutron interaction which correlates the $2s_{1/2}$ and $1d_{3/2}$ proton orbitals with the $1f_{7/2}$ and $2p_{3/2}$ neutron orbitals and leads to appreciable deformation.

In the shell model calculations [2,3] of these nuclei, in particular for the negative parity states (even for the positive parity states of relatively higher spins), one needs a nuclear Hamiltonian over the sd-fp valence space. The Hamiltonian thus consisted of three parts, viz., sd- and fp-shell interactions and the cross-shell ones. Usually the spes used in these Hamiltonians are devoid of the influence of the cross-shell interactions and have to be re-adjusted to reproduce the observed energy spectra. Computational limitations due to large dimensionality problem lead to the truncation of the model space. This may also require an readjustment of the spes. Thus the reduction of the shell gap inferred in [2,3] may have a part which is really due to nucleon-nucleon correlations. The remaining part may be an artifact of other effects connected to the particular truncation scheme involved. This aspect needs more elaborate studies for a definite conclusion.

Thus ^{30}P appears to be an ideal testing ground for studying the onset collectivity within the purview of shell model using effective/empirical (1+2)-body Hamiltonians in a valence space consisting of orbitals from both the sd and fp shells.

^{30}P is perhaps the second nucleus for which complete spectroscopy data are available [6]. The other one being ^{26}Al [7]. Here the term "completeness" means that for a given nucleus, all discrete levels are observed in a specified energy and spin window. These states are all characterized by unique energy, spin, and parity values. In addition, the knowledge of particle and gamma-ray decay branchings is also required for completeness. In ^{30}P data [6], J^π and T have been assigned for more than 100 states up to an excitation energy of 8.00 MeV. However in doing so, some of the ambiguity were eliminated by comparison with the spectrum of ^{30}Si (for $T = 1$ states) and with the shell model spectrum (for positive parity $T = 0$, 1 states). For a few cases parity assignment was ambiguous. Investigation in Ref. [6] did not

*Corresponding author: maitrayee.sahasarkar@saha.ac.in

involve polarization measurement and shell model calculations for negative parity states were also not done. So negative parity was assigned to the states for which there was no prediction for a positive parity state.

This nucleus so far has also been studied [6,8–12] from light particle induced reactions like (p, γ), (α, n), and (α, p) only. Although Endt *et al*. compiled the results obtained from the $^{16}O+^{16}O$ [13] reaction, no detailed publication on these data is found in the literature. The lifetimes of the excited levels of this nucleus have been reported in the literature from the Recoil Distance Method (RDM) and the Doppler Shift Attenuation Method (DSAM) measurements to relatively moderate spins [10–12]. Both shell model and symmetric core collective model calculations have been performed by several groups [10,14,15].

The present study using a Clover array is the first polarization measurement of the gamma rays emitted from the excited states of ^{30}P, populated by the heavy-ion fusion evaporation reaction. We have also investigated the microscopic origin of both positive as well as negative parity states by using shell model results.

II. EXPERIMENT

The experiment was performed at the Tata Institute of Fundamental Research (TIFR), Mumbai, India. This was also one of the first series of experiments performed using the Indian National Gamma Array (INGA) [16] comprised of eight Compton suppressed Clover detectors. The detectors were arranged in the horizontal plane at seven angles of 30, 60, 65, 90, 105, 120, and 145 degrees. The setup is shown in Fig. 1. The solid angle coverage of the setup is $\approx$6% of 4π. The full energy peak efficiency of the array at 1 MeV is $\simeq$1.3%.

A 500 μg/cm^2 ^{24}Mg target with thick Ni backing (sufficient to stop the recoils) was bombarded with the 40 MeV ^{16}O beam provided by the BARC-TIFR Pelletron. A thin layer of oxide (containing ^{nat}O) was present on the surface of the target. The natural abundance of ^{16}O amounts to 99.8%. The nucleus ^{30}P was populated in the $^{16}O(^{16}O,pn)$ reaction. The relative intensities and branching ratios have been calculated from the coincidence data. Although the detector setup does not cover 4π, but as the detectors are arranged more or less symmetrically around the chamber, we have neglected the gamma angular distribution effects. But definitely this has introduced some additional errors in our results. The DCO (directional correlation of oriented states) analysis [17] has been done from the coincident spectra corresponding to 90 and 120 degrees. The experimental R_{DCO} in the present work is defined as

$$R_{DCO} = \frac{I^{\gamma 1}_{90^\circ}(\text{gate on } \gamma_2(120^\circ))}{I^{\gamma 1}_{120^\circ}(\text{gate on } \gamma_2(90^\circ))}. \quad (1)$$

Clover detectors can be used as polarimeters to determine the electric and/or magnetic character of the gamma radiation [18,19]. We have performed integrated polarization asymmetry measurements (IPDCO) [18] by taking all the detectors into consideration. For this purpose two asymmetric IPDCO matrices were constructed corresponding to the parallel and perpendicular projections of the 90° detector. The polarization asymmetry (Δ) is defined as

$$\Delta_{IPDCO} = \frac{a(E_\gamma)N_\perp - N_\parallel}{a(E_\gamma)N_\perp + N_\parallel}, \quad (2)$$

where $N_\perp$ and $N_\parallel$ are the intensities of the full energy peaks observed in perpendicular and parallel matrices, respectively. $a(E_\gamma)$ is the correction term due to asymmetry in the response of the crystals of the Clover detector at 90°. The details of the procedure are discussed in Ref. [2]. Usually pure electric and magnetic natures of radiations yield positive and negative values, respectively, for Δ_{IPDCO}. But for mixed transitions, the sign of the ratio varies depending on the extent of mixing.

FIG. 1. (Color online) INGA setup comprising of eight Clover detectors at TIFR.

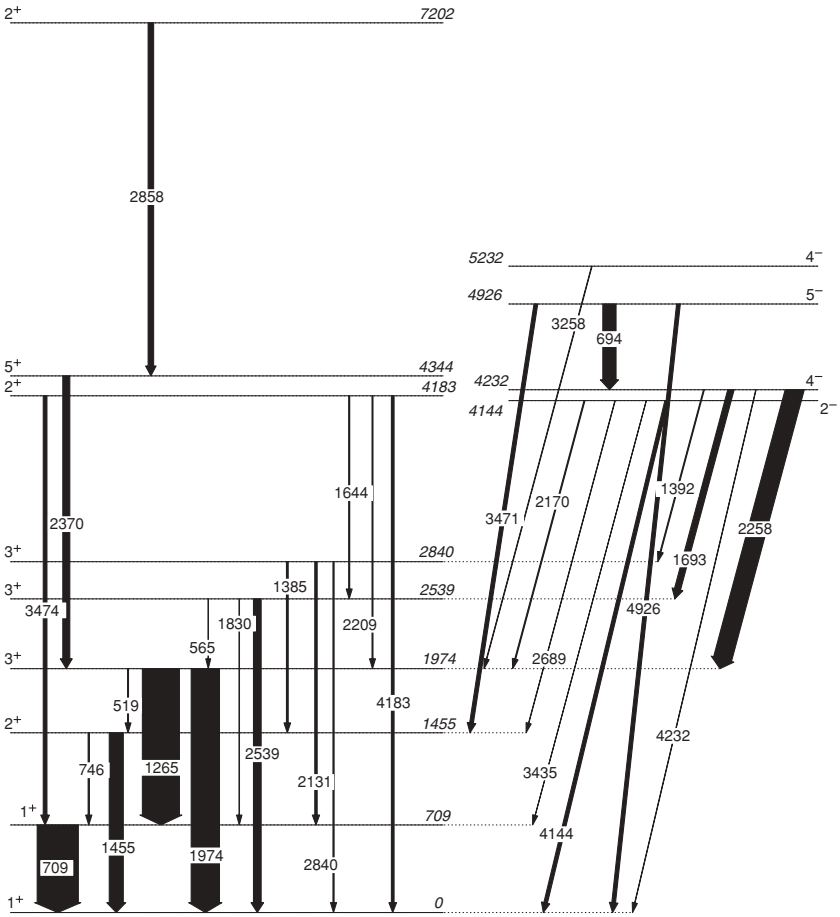

FIG. 2. Partial level scheme of ^{30}P populated in the present work.

The measured asymmetry Δ is related to the degree of polarization $P(\theta)$ by the relation

$$P(\theta) = \frac{\Delta}{Q}, \tag{3}$$

where Q is the polarization sensitivity of the polarimeter. Q depends on the energy of the gamma ray and the geometry of the polarimeter [18,19]. We have calculated the theoretical values of $P(\theta)$ for each of the transitions [18]. The attenuated A_2 and A_4 values have been theoretically estimated [20] by using the known values of spins, parities of the initial and final states, and the spin alignment factor. The correction factor for the finite solid angle of the Clover detector has also been considered [21]. The mixing ratios for the transitions are taken from the present work or from Ref. [22]. The theoretical $P(\theta)$ has been then multiplied by $Q(E_\gamma)$ to get the theoretical value of Δ. We have used the energy dependence of $Q(E_\gamma)$ for the Clover detector from a previous work by Palit *et al.* [19] done in a similar setup.

III. EXPERIMENTAL RESULTS

The partial level scheme obtained from the present experiment is shown in Fig. 2. The relative intensities of the gamma transitions are indicated by the widths of the arrows representing those transitions in the figure. The 709 keV transition is the ground state transition. So we can only assign a lower limit for its intensity. It is equal to the sum of the intensities feeding the 709 keV level. Figure 3 shows two representative gated spectra.

The branching ratios determined from the present work are presented in Tables I and II. The results agree with the

TABLE I. Comparison of experimental branching ratios (present and previous) of the positive parity states with the theoretical calculations (Theo. I).

E_x (keV)	J_i^π	J_f^π	E_γ (keV)	Branching ratio		
				Previous[a]	Present	Theoretical
1455	2^+	1^+	746	4.6 ± 0.4	9	2.4
		1^+	1455	100 ± 0.4	100	100
1974	3^+	2^+	519	<7.2	3	3.8
		1^+	1265	100 ± 0.6	100	100
		1^+	1974	81.8 ± 0.6	76	71.1
2539	3^+	3^+	565	0.41 ± 0.11	1[a]	0.7
		3^+	1830	3.11 ± 0.21	6	4.3
		3^+	2539	100 ± 0.6	100	100
2840	3^+	2^+	1385	55 ± 4	73	62.3
		1^+	2131	100 ± 4	100	100
		1^+	2840	34 ± 4	47	9.6
4183	2^+	3^+	1644	100 ± 16.4	100[a]	100
		3^+	2209	91.8 ± 16.4	93	820
		1^+	3474	1639.3 ± 32.8		8480
		1^+	4183	252.5 ± 16.4	–	1453

[a]Reference [22].

TABLE II. Comparison of experimental branching ratio of the negative-parity states (present and Ref. [22]) with the theoretical calculations (using Theo. II).

E_x (keV)	J_i^π	J_f^π	E_γ (keV)	Branching ratio		
				Previous[a]	Present	Theoretical
4144	2^-	3^+	2170	<1.1	<1.1[a]	1.09
		2^+	2689	9.6 ± 1.64	10	0.15
		1^+	3435	5.9 ± 1.3	5	34
		1^+	4144	100 ± 4	100[a]	100
4232	4^-	3^+	1392	4.5 ± 0.8	5	179
		3^+	1693	37.8 ± 0.8	34	7439
		3^+	2258	100 ± 1.4	100	100
		1^+	4232	3.6 ± 0.8	2	0.25
4926	5^-	4^-	694	100 ± 1.1	100	100
		2^+	3471	12.7 ± 1.1	6	8.5
		1^+	4926	<0.6	<0.6[a]	$\simeq 0$

[a]Reference [22].

previously reported values for the majority of the transitions. Due to lack of sufficient statistics in the gating transitions, the statistical errors in the present branching ratios are large for a few levels. But as the background (Fig. 3) was quite clean, the approximate errors are ~5% for relative intensities $I_\gamma > 50$, ~10 to 20% for $10 < I_\gamma < 50$, and can be up to 50% for $I_\gamma < 10$. For a few gamma-rays, namely, 565, 1644, 2169, 4144, and 4183 keV the intensities could not be calculated either due to some ambiguity or unavailability of a suitable gating transition. For these cases we have used the corresponding values adopted in the literature [22].

TABLE III. Results of the DCO analysis.

E_x (keV)	E_γ (keV)	R_{DCO}	E_{Gate} (keV)	δ/multipolarity		$J_i^\pi \rightarrow J_f^\pi$ γ-ray
				Gate	γ-ray	
1265	1265	0.91 ± 0.12	709	$0.28^{+0.29}_{-0.22}$	$E2$	$3^+ \rightarrow 1^+$
4926	694	1.12 ± 0.23	1265	$E2$	$0.30^{+0.46}_{-0.20}$	$5^- \rightarrow 4^-$

The results from the DCO measurements are given in Table III. Due to poor statistics in the DCO gates we could study only a few cases.The program ANGCOR [17] has been used to compute the theoretical DCO ratios (R_{DCO}). The width of the substate distribution was taken as $\sigma = 0.3\ J$ [2]. To test the correctness of our choice of σ/J, i.e., the extent of spin alignment in the present case, we have used the R_{DCO} value of the 694 keV transition. The multipolarity and mixing ratio for this transition were already reported in Ref. [22]. In Fig. 4, we have plotted the experimental R_{DCO} value from the present work and have compared it with the theoretical R_{DCO} values calculated as a function of σ/J values. The mixing ratio (δ) from our calculation for $\sigma/J = 0.3$ is 0.30 which compares very well to the reported value of 0.29 ± 0.04. The errors in experimental R_{DCO} value have been reflected in the errors in the mixing ratio δ of the 694 keV transition. The experimental and theoretical values of the R_{DCO} agree reasonably well for most of the transitions. The δ for the 709 keV gamma-ray is not reported in the literature. From the present R_{DCO} analysis we deduce the δ value for 709 keV as $0.28^{+0.29}_{-0.22}$ (Table III). For convenience, we have determined it from a reverse condition. This result is obtained by calculating the R_{DCO} value for 1265 keV transition (which is a pure $E2$ [22]) in the 709 keV

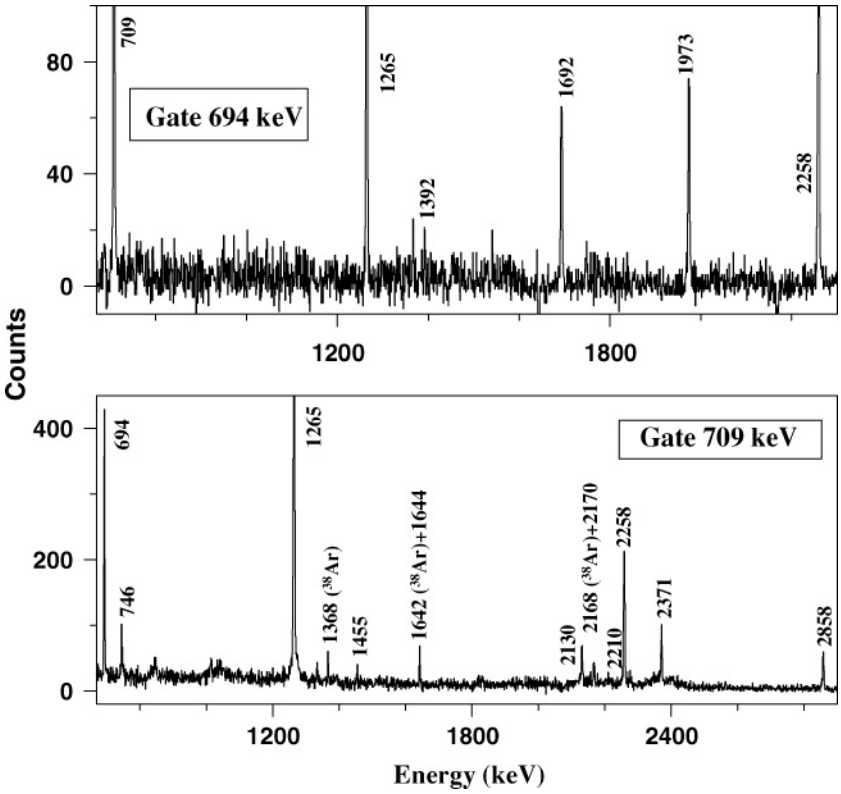

FIG. 3. Representative gated spectra for ^{30}P. The corresponding gating transition is indicated in each spectrum.

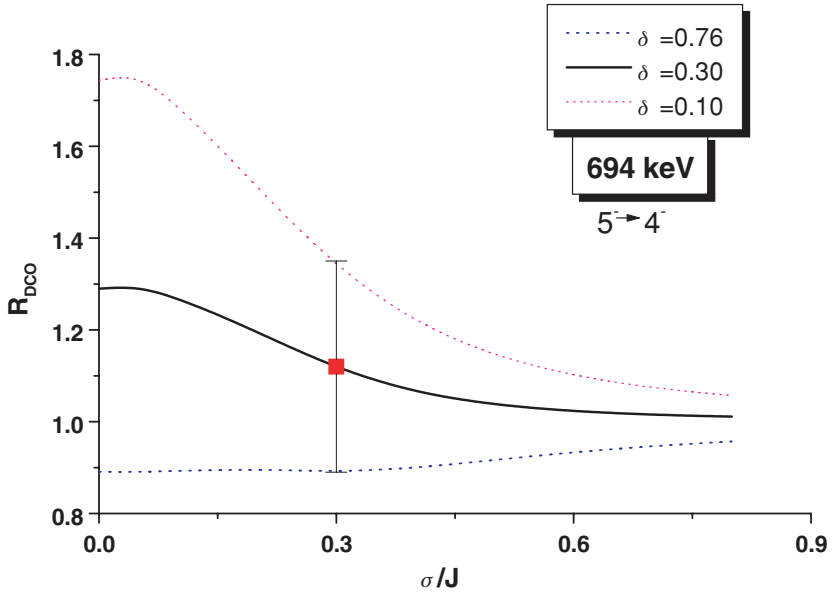

FIG. 4. (Color online) The R_{DCO} values are plotted as a function of the spin alignment factor σ/J for the 694 keV, $5^- \rightarrow 4^-$ transition. The experimental $R_{DCO} = 1.12 \pm 0.23$ is marked on the graph. For $\sigma/J = 0.3$, the errors in the experimental R_{DCO} value have been reflected as the errors in the mixing ratio δ.

gate. The significant quadrupole mixing in 709 keV transition is also supported by the present shell model calculation ($\delta_{theo} = 0.33$) as described later.

The present work reports the first polarization measurement for ^{30}P populated in a heavy-ion fusion reaction. The experimental asymmetry values have been compared with the theoretical estimates of Δ. The results are shown in Fig. 5. Although the experimental asymmetry values have large error bars due to the weak statistics in the polarization spectra, the agreement with theory is quite reasonable for all the transitions. We can see from the figure that the 694 keV transition is of magnetic type.

In the present level scheme (Fig. 2) there are four negative parity states, one each with spin 2 (4144 keV) and 5 (4926 keV) and two with spin 4 (4232 and 5232 keV). To confirm the spins and parities of these states, we have done DCO and polarization measurements. Due to poor statistics in the gated spectra, these measurements can be done for only two transitions deexciting the first 4^- and the 5^- states. The results corresponding to the 694 and 2258 keV gamma transitions support that spin-parity assignments of the states at 4232 and 4926 keV.

IV. THEORETICAL RESULTS AND DISCUSSION

Shell model calculations have been done using the code OXBASH [23]. The valence space consists of ($1d_{5/2}$, $1d_{3/2}$, $2s_{1/2}$, $1f_{7/2}$, $1f_{5/2}$, $2p_{3/2}$, and $2p_{1/2}$) orbitals for both protons and neutrons above the ^{16}O inert core. The number of valence particles (protons + neutrons) in ^{30}P is 14. The "sdpfmw" interaction taken from the Warburton, Becker, Millener, and Brown (WBMB) sd-fp shell Hamiltonian [4] has been used. It consists of Wildenthal's matrix elements for the sd shell, McGrory's Hamiltonian for the fp shell [24], and modification of the Millener-Kurath interaction for the cross-shell components.

Unrestricted calculations with such a large number of valence particles in this model space have often led to

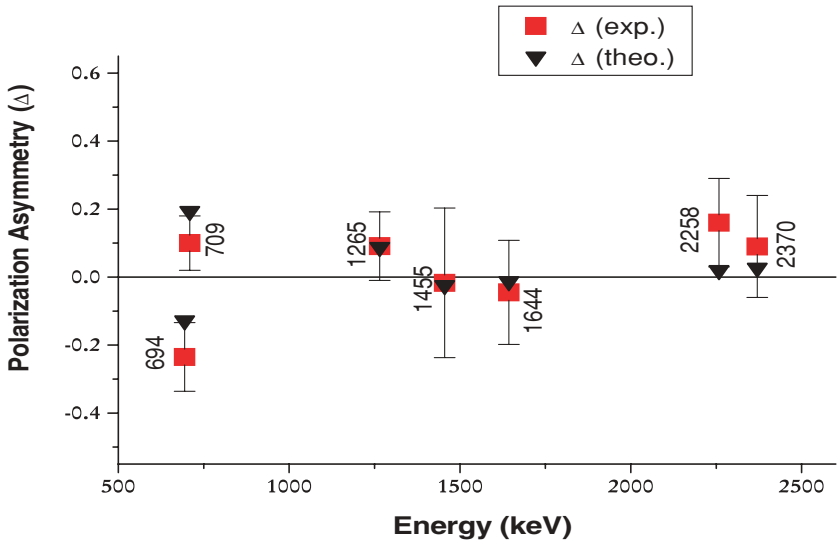

FIG. 5. (Color online) IPDCO values for different gamma rays in ^{30}P. The theoretical value of Δ as discussed in the text has also been marked for each transition. The energies are in keV.

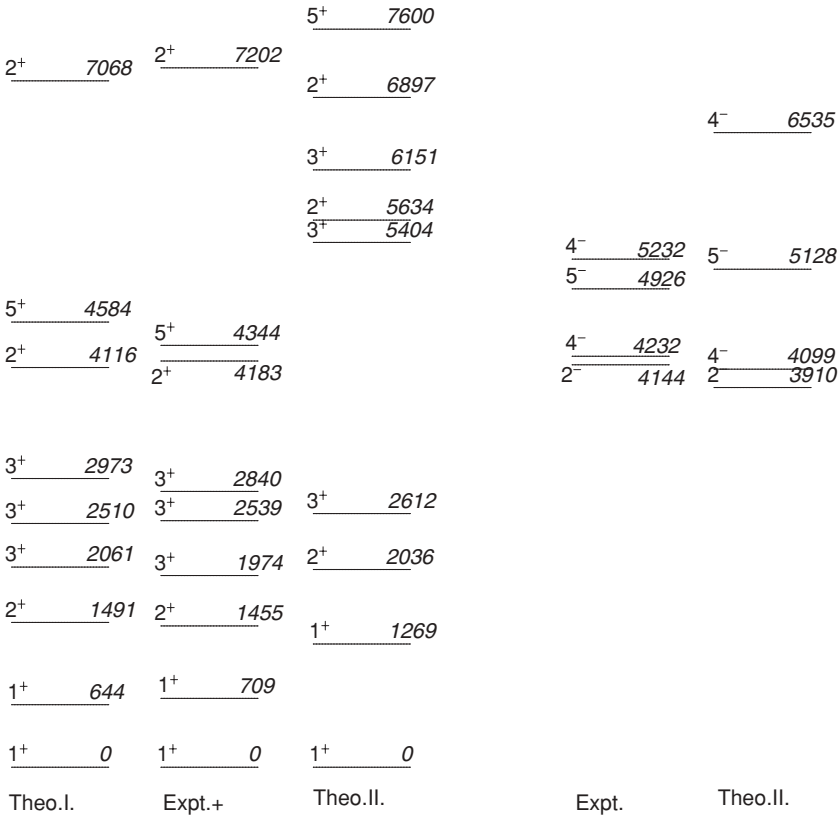

FIG. 6. Experimental level scheme in ^{30}P compared with the shell model results.

prohibitively large m-scheme many-body basis dimensionalities. Several truncation methods [2,3,25–27] have therefore been used for shell model studies of these nuclei. We have also used two truncation schemes in the shell model calculations described below.

A. Truncation scheme I (Theo. I)

In Theo. I (Fig. 6), for the positive parity states, $0\hbar\omega$ excitation has been considered, i.e., only the full sd shell has been used as the valence space. The binding energy of the ground state has been reproduced quite accurately. The theoretical value comes out to be -155.606 MeV, which compares well with the experimental value of -155.657 MeV [28] (corrected for Coulomb energy [29]). The calculated energies of the positive parity states agree quite well with the experimental ones up to 2^+_3 state at 7203 keV. The highest spin observed in this work is $5\hbar$. It is observed that the sd space is sufficient, at least up to this spin. This was also observed in our recent work on ^{35}Cl [2], where the sd space was shown to be adequate up to the $9/2^+$ state. The higher spin states needed the involvement of the orbits from the fp shell. The large deviation of the predicted energies [2] in ^{35}Cl for the higher spin states implied necessarily the insufficiency of the valence space. The nucleon excitations to the neighboring fp shell were therefore essential.

In the calculation of the reduced transition probabilities, the effective charges $e_p = 1.5e$, $e_n = 0.5e$ and the free values of g-factors are used. The calculated branching ratios of the positive parity states and the reduced transition probabilities $B(E2)$ are also compared with the corresponding experimental values (Tables I and IV). The agreement is remarkably good in most cases. As already discussed before, we have also calculated the mixing ratio for the 709 keV ($1^+ \rightarrow 1^+$), $E2/M1$ transition. The theoretical value 0.33 agrees reasonably well with the central value of the measured mixing ratio of $0.28^{+0.29}_{-0.22}$ (Table III).

1. Configuration mixing and collectivity

When the energy difference between the single particle levels is comparable to their two-body interaction terms, those levels are filled up simultaneously. Similarly when the nondiagonal two-body interaction matrix elements connecting different configurations are compared to their energy differ-

TABLE IV. Comparison of experimental and theoretical (using Theo. I) $B(E2)$ values.

E_x (keV)	E_γ (keV)	$B(E2)$ W.u.	
		Adopted [22]	Theoretical
1974	1265	9.0 ± 3.0	11.5
	1974	0.8 ± 0.3	0.87
2539	1830	1.07 ± 0.14	1.83
	2539	6.7 ± 0.8	8.34
2840	2131	2.5 ± 0.4	1.86
	2840	0.20 ± 0.04	0.04

ences, a configuration mixing takes place. In the transition from single particle structure to collectivity, correlations between identical nucleons and nonidentical ones play an important role. Configuration mixed states arising due to pairing correlations between like nucleons are essentially spherically symmetric. Configuration mixing with appropriate neutron-proton correlations is the only plausible way of generating deformation and collectivity [30].

Therefore, to investigate the manifestation of collectivity, the structure of the wave functions should be carefully analyzed. The $B(E2)$ values are also sensitive measures of collectivity. $B(E2)$ values substantially larger than the Weisskopf estimate indicate a collective behavior. The decomposition of the wave functions are shown in Table V. N gives the total number of partitions, each of which contribute more than 1% in the wave function. A general particle partition is, for example, $(j_1^{m_1} \otimes j_2^{m_2} \ldots \otimes j_n^{m_n})$, where $m_1 + m_2 + \ldots + m_n = m$, m being the total number of valence particles. A particle partition may have many different configurations due to various intermediate coupling of angular momenta and isospins. The probability and the structure (i.e., $\{m_1, m_2 \ldots m_n\}$) of partitions with $\geqslant$10% contribution are shown in the table. The partitions are given in terms of occupation numbers of single particle valence states in the following order $1d_{5/2}$, $1d_{3/2}$, $2s_{1/2}$, $1f_{7/2}$, $1f_{5/2}$, $2p_{3/2}$, $2p_{1/2}$. The results are arranged in ascending order with respect to the spin value (I) for positive and negative parity states, respectively. For a particular value of I^π, the indices are assigned according to the partial level scheme shown in Fig. 2. In the adopted level scheme [22], in most cases, there are many other states of the same spin in between.

The low spin (1^+ to 5^+) positive parity states in the full sd shell calculations (Theo. I) show substantial configuration mixing. About 15–18 particle partitions, each having at least 1% contribution, mix. As discussed above, each of these partitions can have different configurations corresponding to several intermediate couplings. The largest contribution from a single partition ranges from 18 to 34%. These wave functions can be compared with those [2] for the positive parity states in ^{35}Cl which is only five nucleons away from doubly closed ^{40}Ca. The yrast positive parity states in ^{35}Cl have a much smaller extent of configuration mixing. For those states, the largest contribution from a single partition is in the range $\simeq$40%–70%. As ^{30}P lies nearly at the mid-sd shell with 49 n-p pairs in the valence space, collectivity manifested in terms of large configuration mixing is expected in this nucleus. This expectation is also consistent with the theoretical studies by Ascuitto *et al.* [15], where a deformation (β) value of 0.15 was used to interpret the excitation spectrum of ^{30}P within the purview of a symmetric core collective model.

The results for transition probabilities (Tables I and IV) also show remarkably good agreement in most of the cases providing a strong evidence in favor of the reliability of the calculated wave functions. Calculated $B(E2)$ values expressed in Weisskopf units (W.u.) are shown in Table IV. It can be seen that only for $3_1^+ \rightarrow 1_2^+$ and $3_2^+ \rightarrow 1_1^+$ transitions, the $B(E2)$ values are relatively larger than the single particle estimates. For states with a high degree of collectivity, $B(E2)$ values are, in general, much larger than these [1,22]. The $B(E2)$ value depends on the reduced matrix element—which is expressed as a sum over one-body transition densities (OBTD) times the reduced single particle matrix elements (RSPME) of the $E2$ operator. A detailed examination of the transition matrix elements reveals that only for these two transitions all the products of OBTDs and RSPMEs are in phase and they add constructively. For all other transitions, some of the product terms have opposite phases and consequent cancellations lead to small $B(E2)$ values.

Calculations are performed in the full sd space and predict the energy eigenvalues and branching ratios quite satisfactorily. So no dramatic change in the single particle structure is expected. The $B(E2)$ values (Table IV) for the transitions connecting the positive parity states indicate a certain degree of coherence in the configuration mixing in the structure of these states. Manifestation of this coherence may be regarded as an onset of collectivity. But it seems that the n-p correlation is not strong enough in this nucleus at least for these states under consideration, to generate a large deformation.

B. Truncation scheme II (Theo. II)

While calculating the energy eigenvalues of the negative parity states we found that unlike in ^{35}Cl [2], the inclusion of the fp shell even in the $1\hbar\omega$ approximation is computationally difficult for this nucleus. So we opted for a different truncation scheme. We carefully analyzed the wave functions of the positive parity states in the full sd space. We found that in most cases the dominant contributions are from partitions having the $1d_{5/2}$ occupancy between 10–12. So in Theo. II, the $1d_{5/2}$ orbital is always constrained to have 10–12 nucleons. In this truncation scheme fp orbitals have been included. But because of the computational limitations we have excluded the high lying $1f_{5/2}$ and $2p_{1/2}$ orbitals from the fp valence space. 0–2 nucleons have been allowed to be in each of the $1f_{7/2}$ and $2p_{3/2}$ orbitals. However, a shell model calculation over this extended space could not provide reasonable results for the eigenvalues of the negative parity states. The energy eigenvalues for the negative parity states are overpredicted. So following our experiences for ^{35}Cl [2], ^{36}S, and ^{34}P in Ref. [3], we have lowered the single particle energies of $1f_{7/2}$ and $2p_{3/2}$ orbitals by 4.5 MeV (Theo. II).

The energy eigenvalues for positive parity states systematically shift to higher energies compared to that in Theo. I. This is expected as we have excluded the partitions which have more than two holes in the $1d_{5/2}$ orbital. As a result, the extent of the configuration mixing also decreases substantially. For Theo. II, partitions involving contributions from the fp shell are also shown in Table V, although they contribute less than 10%. For the positive parity states, they contribute negligibly as shown in the table.

The calculated energies of negative parity states are compared with experiments in Fig. 6 and the wave functions are tabulated in the lower portion of the Table V. In our experiment, ^{30}P was weakly populated. We observed only four negative parity states. They belong primarily to the $\pi\nu(1d_{3/2}1f_{7/2})$ (2^-, 3^-, 4^-, and 5^-) multiplet. Moreover, two more states (3^- and 4^-) arising from $\pi\nu(2s_{1/2}1f_{7/2})$ are also possible. We have

TABLE V. Structure of the wave functions. The partitions are given in terms of occupation numbers of single particle valence states in the following order $1d_{5/2}$, $1d_{3/2}$, $2s_{1/2}$, $1f_{7/2}$, $1f_{5/2}$, $2p_{3/2}$, $2p_{1/2}$. See text for details.

I^π	Energy (MeV)			Wave functions					
	Expt.	Theory		Theo. I			Theo. II		
		Theo. I	Theo. II	%	Partition	N	%	Partition	N
1_1^+	0.0	0.0	0.0	34	[12,0,2]	13	42	[12,0,2,0,0,0,0]	8
	(−)	(−155.607)	(−154.397)	10	[12,1,1]		28	[12,1,1,0,0,0,0]	
				14	[10,2,2]		10	[10,2,2,0,0,0,0]	
							1	[11,0,1,2,0,0,0]	
1_2^+	0.709	0.644	1.269	24	[12,1,1]	18	36	[12,1,1,0,0,0,0]	11
							21	[12,0,2,0,0,0,0]	
							1	[12,0,0,2,0,0,0]	
							1	[10,1,1,2,0,0,0]	
2_1^+	1.455	1.491	2.036	33	[12,1,1]	15	63	[12,1,1,0,0,0,0]	9
				12	[11,2,1]		11	[11,2,1,0,0,0,0]	
							2	[10,1,1,2,0,0,0]	
2_2^+	4.182	4.113	5.634	15	[11,2,1]	16	26	[11,1,2,0,0,0,0]	11
				12	[11,1,2]		23	[11,0,3,0,0,0,0]	
				10	[9,2,3]		14	[11,2,1,0,0,0,0]	
							2	[10,1,1,2,0,0,0]	
							1	[10,0,2,2,0,0,0]	
							2	[11,1,0,2,0,0,0]	
							2	[11,0,1,2,0,0,0]	
2_3^+	7.203	7.068	6.897	22	[10,2,2]	16	31	[11,2,1,0,0,0,0]	10
				12	[9,3,2]		28	[12,1,2,0,0,0,0]	
				10	[10,3,1]		2	[10,1,1,2,0,0,0]	
							1	[11,0,1,2,0,0,0]	
3_1^+	1.974	2.061	2.612	15	[12,2,0]	17	65	[12,2,0,0,0,0,0]	9
				13	[11,0,3]		2	[10,2,0,2,0,0,0]	
							1	[11,1,0,2,0,0,0]	
3_2^+	2.539	2.510	5.404	33	[11,0,3]	18	48	[11,0,3,0,0,0,0]	11
				13	[11,1,2]		16	[11,2,1,0,0,0,0]	
				11	[9,2,3]		11	[10,1,3,0,0,0,0]	
				10	[12,2,0]		1	[10,1,1,2,0,0,0]	
							2	[10,0,2,2,0,0,0]	
							3	[11,0,1,2,0,0,0]	
3_3^+	2.840	2.973	6.151	33	[11,0,3]	18	48	[11,1,2,0,0,0,0]	11
				13	[11,1,2]		15	[11,3,0,0,0,0,0]	
				11	[9,2,3]		11	[10,2,2,0,0,0,0]	
				10	[12,2,0]		1	[10,1,1,2,0,0,0]	
							1	[10,2,0,2,0,0,0]	
							3	[11,1,0,2,0,0,0]	
5_1^+	4.344	4.584	7.600	18	[11,0,4]	16	42	[11,1,2,0,0,0,0]	11
				17	[11,1,2]		15	[10,2,2,0,0,0,0]	
				13	[10,2,2]		13	[11,2,1,0,0,0,0]	
							12	[10,0,4,0,0,0,0]	
							2	[10,0,2,2,0,0,0]	
							2	[10,1,1,2,0,0,0]	
							2	[12,0,0,2,0,0,0]	
							1	[11,0,1,2,0,0,0]	
2_1^-	4.144	–	3.910				67	[12,1,0,1,0,0,0]	9
							11	[10,3,0,1,0,0,0]	
3_1^- [22]	4.626	–	4.609				35	[12,1,0,1,0,0,0]	10
							29	[12,0,1,1,0,0,0]	
3_2^- [22]	6.095	–	6.201				32	[12,1,0,1,0,0,0]	9
							29	[12,0,1,1,0,0,0]	
							12	[11,1,1,1,0,0,0]	

TABLE V. *(Continued.)*

I^π	Energy (MeV)			Wave functions					
	Expt.	Theory		Theo. I			Theo. II		
		Theo. I	Theo. II	%	Partition	N	%	Partition	N
4_1^-	4.232	–	4.099				58	[12,0,1,1,0,0,0]	9
							13	[10,2,1,1,0,0,0]	
4_2^-	5.232	–	6.535				55	[12,1,0,1,0,0,0]	8
							10	[10,3,0,1,0,0,0]	
5_1^-	4.926	–	5.128				66	[12,1,0,1,0,0,0]	7
							11	[10,3,0,1,0,0,0]	

not observed any 3^- level. This may be due to poor statistics. But in the adopted level scheme [22], two 3^- levels have been reported in this energy range. We have included them in our table to complete the comparison for all members of the two multiplets. The agreement of the calculated energy eigenvalues for these negative parity states is quite reasonable except for the 4_2^- state. The branching ratios are also calculated for these negative parity states. We have already pointed out that there is a large disagreement between the energy eigenvalues for the positive parity relatively higher spin ($>2^+$) states for Theo. II. Although the theoretical and experimental branching ratios (Table II) agree for most of the negative parity states, only that for the 4_1^- (4232 keV) state is not satisfactory. This may be due to the fact that the extent of the mixing between the two 4^- states arising from two different multiplets is not reproduced correctly. This is therefore reflected in the disagreement for the energy of 4_2^- and branching ratios of 4_1^-. Unsatisfactory reproduction of the final states, i.e., the positive parity ones (Theo. II), might be another reason that led to this result.

V. CONCLUSION

^{30}P has been populated in a heavy ion fusion evaporation reaction up to moderate spins ($I = 5$). The first polarization measurement for this nucleus has been done in this work. It confirms the spin-parity assignments of a few levels up to about 7 MeV. Positive parity states are well described within the full sd-space shell model calculation. The onset of collectivity for the positive parity states in terms of coherence in the mixing of configurations has been indicated. But n-p correlations are not strong enough to generate substantial deformation. Calculations in the truncated sd-fp space have also been done for both the negative and positive parity states. The energy eigenvalues of the negative parity states are reasonably reproduced when the sd-fp shell gap is reduced by about 4.5 MeV. These states originate primarily from the π-ν multiplet structures. The eigenvalues of the positive parity states (Theo. II) are overpredicted due to the truncation used. More heavy ion data at higher excitation energies are needed to study the extent of collectivity developed at higher spins.

ACKNOWLEDGMENTS

The authors thank the members of the INGA collaboration for their help and support, Pradipta Das for help in target preparation, and the Pelletron staffs of TIFR for providing the beam.

[1] C. E. Svensson *et al.*, Phys. Rev. Lett. **85**, 2693 (2000); E. Ideguchi *et al.*, *ibid.* **87**, 222501 (2001); C. E. Svensson *et al.*, Phys. Rev. C **63**, 061301 (2001); E. Caurier, F. Nowacki, and A. Poves, Phys. Rev. Lett. **95**, 042502 (2005).
[2] Ritesh Kshetri *et al.*, Nucl. Phys. **A781**, 277 (2007), and references therein.
[3] Krishichayan *et al.*, Eur. Phys. J. A **29**, 151 (2006), and references therein.
[4] E. K. Warburton, J. A. Becker, and B. A. Brown, Phys. Rev. C **41**, 1147 (1990).
[5] E. Caurier, K. Langanke, G. Martinez-Pinedo, F. Nowacki, and P. Vogel, Phys. Lett. **B522**, 240 (2001).
[6] C. A. Grossmann, M. A. LaBonte, G. E. Mitchell, J. D. Shriner, J. F. Shriner, G. A. Vavrina, and P. M. Wallace, Phys. Rev. C **62**, 024323 (2000).
[7] P. M. Endt, P. de Wit, and C. Alderliesten, Nucl. Phys. **A459**, 61 (1986); **A476**, 333 (1988).
[8] G. I. Haris *et al.*, Phys. Rev. **157**, 958 (1967).
[9] J. P. L. Reinecke *et al.*, Nucl. Phys. **A435**, 333 (1985).
[10] P. Tikkanen, J. Keinonen, R. Lappalainen, and B. H. Wildenthal, Phys. Rev. C **36**, 32 (1987).
[11] E. F. Kennedy *et al.*, Phys. Rev. **158**, 897 (1967).
[12] F. Haas *et al.*, Nucl. Phys. **A156**, 385 (1970).
[13] P. M. Endt, Nucl. Phys. **A521**, 1 (1990).
[14] P. M. Endt and J. G. L. Booten, Nucl. Phys. **A555**, 499 (1993).
[15] R. J. Ascuitto *et al.*, Phys. Rev. **176**, 1323 (1968).
[16] H. C. Jain, Pramana **57**, 21 (2000).
[17] K. S. Krane and R. M. Steffen, Phys. Rev. C **2**, 724 (1970).
[18] G. D. Jones, Nucl. Instrum. Methods A **491**, 452 (2002); K. Starosta *et al.*, *ibid.* **423**, 16 (1999); T. Aoki, K. Furuno, Y. Tagishi, S. Ohya, and J.-Z. Ruan, At. Data Nucl. Data Tables **23**, 349 (1979).
[19] R. Palit, H. C. Jain, P. K. Joshi, S. Nagaraj, B. V. T. Rao, S. N. Chintalapudi, and S. S. Ghugre, Pramana **54**, 347 (2000).
[20] E. Der Mateosian and A. W. Sunyar, At. Data Nucl. Data Tables **13**, 391 (1974).
[21] K. S. Krane, Nucl. Instrum. Methods **98**, 205 (1972).
[22] http://www.nndc.bnl.gov.

[23] B. A. Brown, A. Etchegoyen, W. D. M. Rae, and N. S. Godwin, MSU-NSCL Report No. **524**, 1985 (unpublished).
[24] J. B. McGrory, Phys. Rev. C **8**, 693 (1973).
[25] M. Ionescu-Bujor *et al*., Phys. Rev. C **73**, 024310 (2006).
[26] A. Kangasmaki, P. Tikkanen, J. Keinonen, W. E. Ormand, S. Raman, Zs. Fulop, A. Z. Kiss, and E. Somorjai, Phys. Rev. C **58**, 699 (1998); A. Kangasmaki, P. Tikkanen, J. Keinonen, W. E. Ormand, and S. Raman, *ibid*. **55**, 1697 (1997).
[27] P. Mason *et al*., Phys. Rev. C **71**, 014316 (2005).
[28] G. Audi, A. H. Wapstra, and C. Thibault, Nucl. Phys. **A729**, 337 (2003).
[29] B. J. Cole, J. Phys. G **11**, 351 (1985).
[30] Dorin N. Poenaru and Walter Greiner, *Handbook of Nuclear Properties* (Oxford University Press, Oxford, 1996), p. 39; R. F. Casten, *Nuclear Structure from a Simple Perspective* (Oxford University Press, Oxford, 1990), p. 141.